XLI CILAMCE
XLI Ibero-Latin American Congress on Computational Methods in Engineering
16-19 November, 2020 FOZ DO IGUAÇU PARANÁ - BRAZIL

Numerical approximation of the classical solutions for plates

Matheus S. Carvalho[1], Jorge C. Costa[1]

[1]*Dept. of Civil Engineering, Federal University of Sergipe*
Rod Marechal Rondom, SN, 49.100-000, São Cristóvão, Sergipe, Brazil
matheuss020@gmail.com, jorgecostase@gmail.com

Abstract. This article proposes a solution, obtained by line adjustment, to the problem of bending of thin plates with small deflections. The aim of this solution is to make the programming and manual calculation of bending moments and deflections easier than classical method equations and calculation tables. The values to make the fit was obtained by programing the Levy's classical method in MATLAB® and the results were close to the values given by Timoshenko e Goodier (1959). The line adjustment was made in MATLAB® and the shape function was a polynomial equation of third degree with four variables. Furthermore, the values obtained numerically was compared with the coefficients in Chust and Figueiredo's (2014) calculations table. It was verified that the tabulated values were not the maximums because they were always obtained in the middle of the plate. Therefore, a new calculation table for each kind of plate with the maximum values is proposed along with closed form approximations. The analyses were carried out for rectangular plates with clamped or simply supported edges.

Keywords: Classical theory of plates, thin rectangular plates, calculation tables, bending moments, deflections.

1 Introduction

Thin plates are bidimensional structures with one of the dimensions, the thickness, significantly smaller than the two others. Usually, the ratio between the two smallest dimensions of a plate is no larger than $1/10$. As such, bidimensional plate theories are sufficient to analyze small deflections caused by loading, as long as the deflections remain small.

The classical methods were the first developed to analyze plate bending, especially with the advent of reinforced concrete slabs. They are based on algebra and differential calculus to describe the mechanics and provide satisfactory analytical solutions for most usual plate shapes and loadings.

Nevertheless, those methods provide solutions in the form of trigonometrical series and, for that reason, both manual calculations and computer programming are not straightforward or easily accomplished. This resulted in many calculation tables being created to summarize the values obtained by these methods in order to simplify hand-made analysis. These calculation tables became the standard practice [1] for concrete slab design, at least before the dissemination of computer-based solutions such as matrix solution of grids or finite elements.

Early efforts to make these calculations automatic would look towards an algorithm based on searching these tables. Besides being inefficient and unpractical, it would imply a rework since they already come from a simplification and numerical solution.

In this context, there are presently two options for slab analysis: manual calculations with the help of tables, or numerical methods such as finite elements. Hence, this work proposes an intermediary solution based on classical methods that can be used on hand calculations and easily programmable. This way, this solution can be inserted in automated analysis routines of slabs with no need to resort to tables or numerical methods.

In this work, italic letters $(a, b, \alpha, \beta, \dots)$ represent scalar. Especially, w will always stand for plate deflection, D for plate stiffness in many forms, q for the load, ν for Poisson's ratio, a, b for the plate larger dimensions, h for thickness and E for the Young modulus of concrete. A Cartesian reference system will be used with the plate's midsurface in the $x \times y$ plane and thickness in the z direction.

2 Classical solutions

Efforts to mathematically model the behavior of plates remount to the works of Leonhard Euler (1707-1783), Jacques Bernoulli (1759-1789), Ernst Chladni (1756–1827), Sophie Germain (1776-1831), Joseph-Louis Lagrange (1736-1813), Siméon Poisson (1781-1840) and others [2, 3, 4].

The first complete model for plate bending can be attributed to Navier in 1820. This solution consisted of using a double Fourier trigonometric series to approximate the load imposed on the plate and consequently its transversal displacement. Latter, Maurice Levy (1839-1910) introduced as a solution a single trigonometric Fourier series for plates with two opposing sides simply supported and the remaining sides either free or also simply supported [2].

The nomenclature for the plates will follow Reddy [5] and is represented in Fig.1. Also, the x axis will always be parallel to the smaller side, with dimension a, and the y axis will be parallel to the larger dimension b. We emphasize that the ratio between the plate sizes will be represented by $\lambda = b/a$ and that the plates will be analyzed under uniform distributed load q_o, the most common situation for the structural analysis of civil engineering structures.

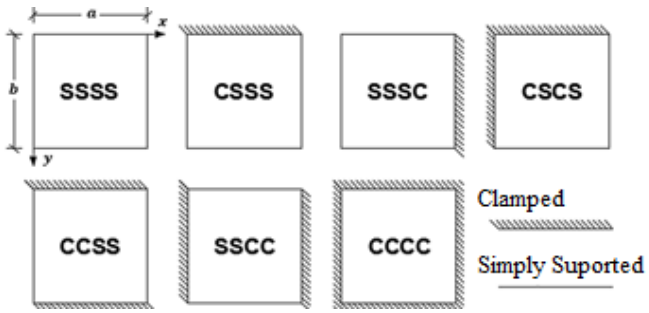

Figure 1. Plate nomenclature.

2.1 Navier's Method

According to Timoshenko and Goodier [6], Navier, analyzing the plate equilibrium represented by the differential equation

$$D\left(\frac{\partial^4 w}{\partial x^4\,\partial} + 2\frac{\partial^4 w}{\partial x^2\,\partial y^2} + \frac{\partial^4 w}{\partial y^4}\right) = q, \tag{1}$$

noticed that this equation admits a relatively trivial solution for trigonometric loads such as

$$q_{mn} = a_{mn}\, sen\frac{m\pi x}{a} sen\frac{n\pi y}{b} \rightarrow w_{mn} = b_{mn} sen\frac{m\pi x}{a} sen\frac{n\pi y}{b}. \tag{2}$$

Consequently, if a loading can be approximated by a series of q_{mn}, the displacements would result in another series.

$$q = \sum_{m=1}^{\infty}\sum_{n=1}^{\infty} a_{mn}\, sen\frac{m\pi x}{a} sen\frac{n\pi y}{b} \rightarrow w = \sum_{m=1}^{\infty}\sum_{n=1}^{\infty} b_{mn} sen\frac{m\pi x}{a} sen\frac{n\pi y}{b} \tag{3}$$

In the case of SSSS plates such as depicted in Fig.2, the boundary conditions are

$$\begin{aligned} w = 0\,;\ \frac{\partial^2 w}{\partial x^2} = 0, \text{for } x = 0 \text{ and } x = a, \\ w = 0\,;\ \frac{\partial^2 w}{\partial y^2} = 0, \text{for } y = 0 \text{ and } y = b. \end{aligned} \tag{4}$$

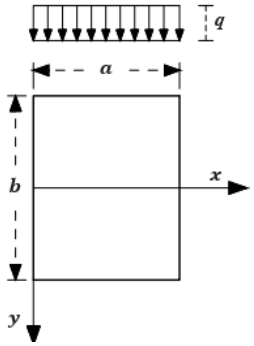

Figure 2. Navier's SSSS Plate.

A uniform load q_o can be approximated by

$$q = \sum_{m=1}^{\infty}\sum_{n=1}^{\infty} \frac{16q_o}{\pi^2 mn}\, sen\frac{m\pi x}{a} sen\frac{n\pi y}{b}, \tag{5}$$

so that the deflection is obtained as

$$w = \frac{16q_0}{\pi^6 D}\sum_{m=1}^{\infty}\sum_{n=1}^{\infty} \frac{sen\frac{m\pi x}{a} sen\frac{n\pi y}{b}}{mn\left(\frac{m^2}{a^2}+\frac{n^2}{b^2}\right)^2}. \tag{6}$$

Other quantities such as moments and shear stresses can be obtained from the deflection.

2.2 Lévy's Method

According to Timoshenko and Goodier [6], Levy proposed a solution in the form of

$$w = w_1(x) + w_2(x,y). \tag{7}$$

The w_1 part is inspired by the deflection of a beam in the x direction in such a way as to comply with the boundary conditions on the larger sides

$$w_1 = 0\,;\ \frac{\partial^2 w_1}{\partial x^2} = 0 \text{ for } x = 0 \text{ and } x = a \tag{8}$$

and the non-homogeneous part of the equilibrium equation

$$D\left(\frac{\partial^4 w_1}{\partial x^4} + 2\frac{\partial^4 w_1}{\partial x^2\,\partial y^2} + \frac{\partial^4 w_1}{\partial y^4}\right) = q. \tag{9}$$

Hence, for a uniform load q_o and simply supported longer sides,

$$w_1 = \frac{q_o}{24D}(x^4 - 2ax^3 + a^3 x). \tag{10}$$

Function w_2 must obey a homogeneous equilibrium eq. (13) and also the boundary conditions on the longer sides. Moreover, the sum (7) must obey all the boundary conditions

$$w_2 = 0\,;\ \frac{\partial^2 w_2}{\partial x^2} = 0, \text{ for } x = 0 \text{ and } x = a \tag{11}$$

$$w = w_1 + w_2 = 0;\ \frac{\partial^2 w}{\partial y^2} = \frac{\partial^2 w_2}{\partial y^2} + \frac{\partial^2 w_1}{\partial y^2} = 0, \text{ for } y = 0 \text{ and } y = b \tag{12}$$

$$D\left(\frac{\partial^4 w_2}{\partial x^4}+2\frac{\partial^4 w_2}{\partial x^2\,\partial y^2}+\frac{\partial^4 w_2}{\partial y^4}\right)=0 \tag{13}$$

In this manner, w_2 is proposed as a series (14) where Y_m is only dependent on y

$$w_2=\sum_{m=1}^{\infty} Y_m(y)\,sin\frac{m\pi x}{a}. \tag{14}$$

A. Nadai proposes the Y_m part of the solution as a hyperbolic trigonometric function

$$Y_m=\frac{qa^4}{D}\left(A_m cosh\frac{m\pi y}{a}+B_m\frac{m\pi y}{a}sinh\frac{m\pi y}{a}+C_m sinh\frac{m\pi y}{a}+D_m\frac{m\pi y}{a}cosh\frac{m\pi y}{a}\right), \tag{15}$$

where the constants A_m, B_m, C_m, D_m are chosen as to obey the support conditions. For an SSSS plate C_m, D_m are zeroes as symmetry along the x axis imposes that only even functions are kept. The imposition of the other boundary conditions yields

$$A_m=-\frac{2(\alpha_m tanh\ \alpha_m+2)}{\pi^5 m^5 cosh\,\alpha_m}\ ;\ B_m=\frac{2}{\pi^5 m^5 cosh\,\alpha_m}. \tag{16}$$

Lastly, we arrive at eq. (17), that represents the deflection of an SSSS plate with uniformly distributed load.

$$w=\frac{4q_o a^4}{\pi^5 D}\sum_{m=1}^{\infty}\frac{1}{m^5}\left(1-\frac{(\alpha_m tanh\ \alpha_m+2)}{2\,cosh\,\alpha_m}cosh\frac{2\,\alpha_m y}{b}+\frac{\alpha_m}{2\,cosh\,\alpha_m}\frac{2y}{b}senh\frac{2\,\alpha_m y}{b}\right)sen\frac{m\pi x}{a} \tag{17}$$

2.3 Calculation Tables

The main calculation tables used for the analysis of concrete slabs are those by Bares (1970) with several values for Poisson's ratio; by Kalmanok (1961) with $\nu=0$; and, in Brazil, those by Chust e Figueiredo Filho (2014) with $\nu=0{,}2$ [7].

The tables present coefficients α,μ_x, μ'_x, μ_y and μ'_y used to find the maximum bending moments and deflections through the expressions. The subscript x, y indicates the direction of the fibers being stressed by the moment and M' is the moment at a clamped boundary.

$$\mu_x \text{ or } \mu'_x=\frac{100\,M_x}{q_0 a^2}, \tag{18}$$

$$\mu_y \text{ or } \mu'_y=\frac{100\,M_y}{q_0 a^2}, \tag{19}$$

$$\alpha=\frac{100\,wEh^3}{q_0 a^4}. \tag{20}$$

For an SSSS plate with uniform load, Lévy's solution in eq. (17) renders a maximum transversal displacement of

$$w=\frac{4q_o a^4}{\pi^5 D}\sum_{m=1}^{\infty}\frac{(-1)^{(m-1)/2}}{m^5}\left(1-\frac{(\alpha_m tanh\ \alpha_m+2)}{2\,cosh\,\alpha_m}\right). \tag{21}$$

Using the definition Eq.(20) of α, $\lambda = b/a$ and $\alpha_m = m\pi\lambda/2$, we arrive at

$$\alpha(\lambda)=\frac{48(1-\nu^2)}{\pi^5}\sum_{m=1}^{\infty}\frac{(-1)^{(m-1)/2}}{m^5}\left(1-\frac{(\alpha_m tanh\ \alpha_m+2)}{2\,cosh\,\alpha_m}\right). \tag{22}$$

3 Comparison of the Methods

One approach to comparing the presented methods is through a convergence analysis. Fig.4 depicts the error in displacement for both Navier and Lévy solutions with 1, 2 or 3 terms in the series in respect to the exact (converged) solution for an SSSS plate.

It can be seem that Lévy's solution converge faster than Navier's, as results with 3 terms are already indistinguishable from the reference solution for all the λ analyzed.

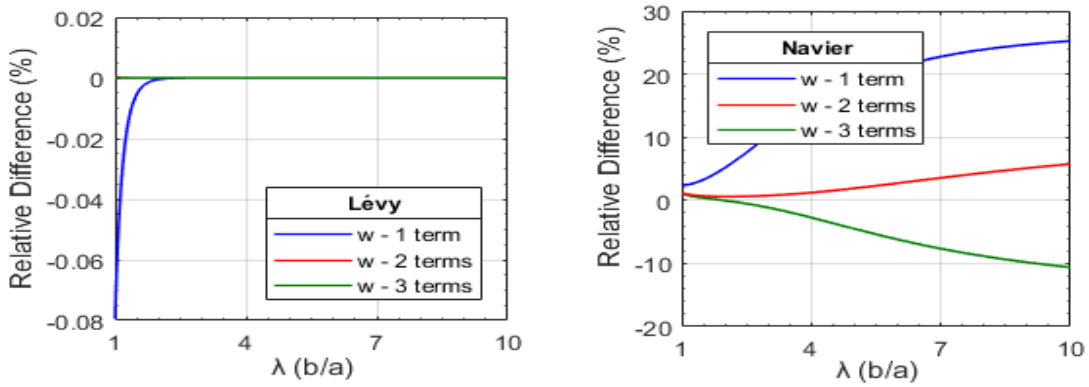

Figure 3. Displacement error for Lévy's and Navier's approximation with 1, 2 and 3 terms

Fig.5 depicts the first term of the series used to approximate the uniform load. It can be noted that Lévy's solution present an excellent approximation for the load even with only one term, whereas Navier's solution do not approximate the load in a satisfactory manner.

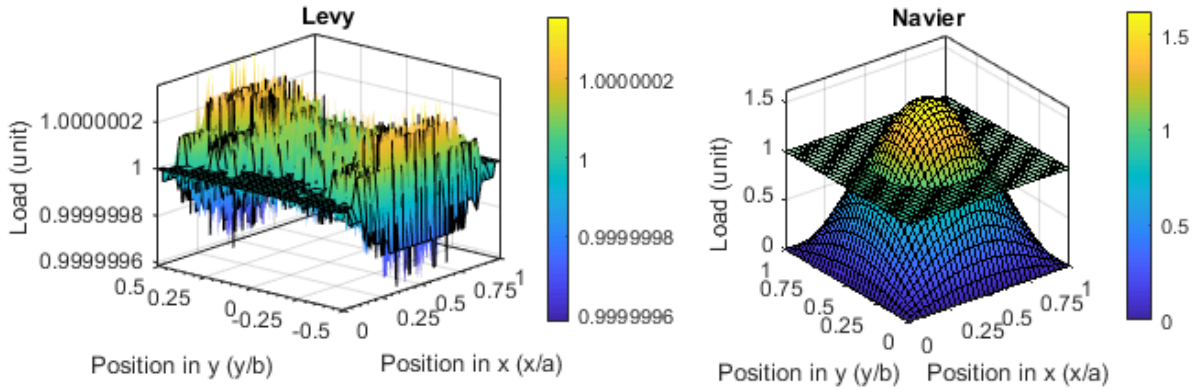

Figure 4. Load representation for the first term of Lévy's and Navier's solutions.

As such, we can verify what is stated by Timoshenko e Goodier [6], that Levy's method is more convenient for computer implementation.

4 Curve Fitting

The equations were approximated using the Curve Fitting Toolbox available in MATLAB®. The methods to evaluate the quality of a fitting are of two kinds. The first are the graphic methods as residue analysis that help on visual interpretation. The second are the numerical methods as quality statistic data and the confidence interval that provide numerical evidence to help the statistical reasoning. The referred toolbox [8] provide data such as the sum of squared errors (SSE), R-square, adjusted R-square and the root mean squared error as depicted in Fig.6.

Results

General model:

f(x) = a*x^3+b*x^2+c*x+d

Coefficients (with 95% confidence bounds):

a = -0.3048 (-0.3344, -0.2752)

b = -1.513 (-1.646, -1.379)

c = 13.66 (13.46, 13.86)

d = -7.169 (-7.263, -7.075)

Goodness of fit:

SSE: 0.03614

R-square: 1

Adjusted R-square: 1

RMSE: 0.008536

Figure 5. Goodness-of-Fit Statistics

5 Results and discussion

5.1 Linear Fitting

Linear fittings were developed as to serve as an alternative to the calculation tables and as to make easier the programming of the values. The objective is to provide a way to obtain the α and μ parameters with no need to calculate Levy's series or resort to calculation tables. The fittings were carried such as to achieve a good quality in the results with the least number of parameters.

$$\mu = a\lambda^3 + b\lambda^2 + c\lambda + d \tag{23}$$

A visual inspection of the curves for coefficients α, μ_x, μ'_x, μ_y and μ'_y motivated the use of 4-parameter 3rd - degree polynomial function approximation as in Eq.(22). In this equation, μ stand for any of the desired parameters. Other approximating functions were considered, such as rational and trigonometrical approximations, nevertheless, the polynomial provided better results. The fitting was carried with 500 points for each parameter in the interval $1 < \lambda < 2$ and a confidence interval of 95%. Poisson's ratio was taken as $\nu = 0{,}2$.

As for the goodness of fit, the values of R-square and Adjusted R-square remain close or equal to 1, what points to a good fit. Moreover, the values of SSE and RMSE remain close to 0, also an indication of a good fit. The observed residues were also close to null, with a random distribution characteristic of a suitable approximation function. The resulting parameters for eq.(23) are reported in Tab.1.

6 Conclusions

It is remarked that the equations obtained through the fitting are a good alternative to calculate maximum deflections and bending moments on concrete slabs. These equations simplify the classical methods and make easier for both manual and automated calculations. Moreover, these equations are easier to be programmed than calculation tables and, for manual calculations, they preclude the use of interpolations and the large number of tables necessary to cover every kind of plate.

This work can be further developed through comparative analyses with other numerical and algebraic methods available in the literature. It is also subject to a better analysis of the fitting procedures, through the use of other approximating functions or mathematical analysis of the series solution of the differential equation.

Acknowledgements. The authors acknowledge the Federal University of Sergipe for the funding of this research.

Authorship statement. The authors hereby confirm that they are the sole liable persons responsible for the authorship of this work, and that all material that has been herein included as part of the present paper is either the property (and authorship) of the authors, or has the permission of the owners to be included here.

Table 1. Fitted coefficients

Plate supports		$1 < \lambda < 2$ $\mu^* = a\lambda^3 + b\lambda^2 + c\lambda + d$				∞
		a	B	c	d	
SSSS	α	-0,3048	-1,513	13,66	-7,169	15,00
	μx	-0,0236	-2,4	12,94	-6,1	12,50
	μy	1,968	-9,346	13,68	-1,872	3,83
CCSS	α	-2,47	10,46	-6,574	0,7825	15,00
	μx	-1,872	7,449	-2,946	-0,4958	12,50
	μy	1,217	-7,695	15,34	-5,704	3,35
	μy'	-1,22	9,674	-25,41	9,986	-12,50
SSCC	α	0,7025	-4,127	8,263	-2,626	3,00
	μx	0,9655	-5,624	11,14	-3,306	4,18
	μx'	-1,743	9,867	-18,84	3,719	-8,33
	μy	-0,932	4,86	-8,459	6,672	1,75
CSSS	α	-1,492	4,698	3,835	-3,759	15,00
	μx	-0,9674	2,411	5,653	-3,927	12,50
	μy	1,873	-9,944	16,75	-4,777	3,64
	μy'	-2,127	13,34	-28,91	9,306	-12,50
SSSC	α	0,8021	-5,609	13,75	-5,657	6,20
	μx	0,9215	-6,322	15,22	-5,926	7,06
	μx'	-1,921	12,1	-26,59	8,02	-12,50
	μy	0,05056	0,6529	-3,038	5,536	1,41
CCCC	α	0,5094	-3,676	8,928	-4,311	3,00
	μx	0,8005	-5,537	12,98	-6,136	4,18
	μx'	-1,779	11,44	-25,04	10,25	-8,33
	μy	1,423	-6,025	7,491	-0,7616	1,49
	μy'	-1,759	9,006	-15,26	2,858	-5,70
CSCS	α	0,3966	-3,934	12,14	-6,041	6,20
	μx	0,5398	-4,792	13,94	-6,606	7,02
	μx'	-1,405	10,46	-26,59	10,77	-12,50
	μy	1,117	-4,931	6,507	0,4269	2,55
	μy'	-2,173	11,38	-19,79	3,793	-7,65
*Where μ may be α, μx, μx', μy or μy'						

References

[1] B. Mosley, J. Bungey and R. Hulse. *Reinforced concrete design to Eurocode 2*. New York: Palgrave Macmillan, 2007.
[2] R. Szilard. *Theory and Analysis of Plates*: classical and numerical methods. New Jersey: Prentice-Hall Inc. New Jersey: John Wiley & Sons, 2004.
[3] S. P. Timoshenko. *History of Strength of Materials*. Mcgraw-Hill Book Company, New York, 1953.
[4] M. C. Santos. *Uma Revisão dos Métodos Clássicos de Análise de Placas*. Graduation dissertation [in Portuguese]. Federal University of Sergipe, São Cristóvão, 2020.
[5] J. N. Reddy. *Theory and Analysis of Elastic Plates and Shells*. 2.ed. New York, 2007.
[6] S. P. Timoshenko and J. N. Goodier. *Theory of Plate and Shells*, Mcgraw-Hill Book Company. 2 ed. Singapure, 1959.
[7] J. M. Araújo. *Curso de concreto armado – volume 2*. 2. ed. [in Portuguese]. Rio Grande do Sul: Dunas, 2010.
[8] MathWorks®. *Evaluating Goodness of Fit*. How to Evaluate Goodness of Fit. Disponível em: <https://www.mathworks.com/help/curvefit/evaluating-goodness-of-fit.html>. Accessed on 05 February 2020.